ELSEVIER

Contents lists available at ScienceDirect

Electric Power Systems Research

journal homepage: www.elsevier.com/locate/epsr



Processes in negative and positive CG lightning flashes detected from space by GLM

Adonis F.R. Leal a,b,*, Vladimir A. Rakov c

- ^a New Mexico Institute of Mining and Technology, 801 Leroy Place, Socorro 87801, United States
- ^b Graduate Program in Electrical Engineering, UFPA, Belem 66075110, Brazil
- ^c University of Florida, 553 Engeniring Bulding, Gainesville 32611, United States

ARTICLE INFO

Keywords:

Negative and positive lightning flashes Electric field waveforms Lightning detection from space

ABSTRACT

Negative and positive lightning flashes involve a number of different processes, including the preliminary breakdown, stepped and dart leaders, return strokes, continuing currents, M-components, etc. The Geostationary Lightning Mapper (GLM) onboard of Geostationary Operational Environmental Satellites (GOES 16, 17 and 18) is an optical lightning detector with a time resolution of 2 ms and spatial resolution of about 8 km at nadir. The GLM provides three types of data: events, groups, and flashes. According to GLM designers, the group data are intended to track individual lightning strokes. We recorded wideband lightning electric fields using fast and slow antennas in the Amazon and compared them with the corresponding GLM group data (optical energy in Joules) to investigate what lightning processes can be detected from space by GLM. Based on a sample of 15 -CG flashes containing 56 strokes and 15 +CG flashes containing 24 strokes, we found that GLM detected some luminosity in 89 % of 2 ms time windows corresponding to -CG return strokes and 96 % of windows corresponding to +CG return strokes. It also detected luminosity in 100 % of time windows corresponding to preliminary breakdown processes in positive flashes versus 53 % in negative flashes. Further, the GLM detected luminosity emissions associated with 80 % and 40 % of first-stroke leaders in positive and negative flashes, respectively. In general, GLM is more efficient in detecting processes in positive lightning flashes than in negative ones.

1. Introduction

Negative and positive cloud-to-ground lightning flashes (-CGs and +CGs) involve a number of different processes, some of which occur (at least in part) outside the cloud, such as leaders initiating first strokes, subsequent-stroke leaders, return strokes, continuing currents, and M-components, while others involve channels that are confined to the cloud such as preliminary breakdown and compact intracloud discharges (CIDs, also known as NBEs) [1,2]. The main difference between -CGs and +CGs is the polarity of charge removed from the cloud: -CGs remove negative charge, while +CGs remove positive charge (usually residing at higher altitudes in the cloud than negative). All the lightning processes are associated with charge motion and, hence, produce electromagnetic fields that can be recorded at ground level.

Lightning also emits electromagnetic waves in the visible range. Those emissions can be detected with optical sensors at ground level and also from space. Optical sensors at ground level are usually high-speed framing cameras, photodiodes, or phototransistors. High-speed

cameras usually operate at wavelengths covering the entire (or most of the) visible range. On the other hand, photodiodes and phototransistors are good tools for recording emissions with specific wavelengths using appropriate lenses and filters [3,4]. Recently, the Geostationary Lightning Mapper (GLM) onboard the Geostationary Operational Environmental Satellites (GOES 16, 17 and 18) started its operation. GLM detects lightning by looking for transient optical pulses at the 777.4-nm wavelength [5]. The GLM has a sampling rate of 500 frames per second and each pixel permits a consistent resolution of ~8 km across most of its field of view and increases to 14 km near its edge [5]. The GLM was designed to detect >70 % of all flashes when averaged over 24 hrs, with better performance at night (\sim 90 %) than during the day (\sim 70 %) [5,6]. In central Florida, GLM (on GOES-16) flash detection efficiency (DE) was found to be 73.8 % [7]. For the entire field of view of GLM (on GOES 16) the average DE is 97 % for a coincidence time window of ± 10 min, and for the period between August 1, 2019 and January 31, 2020 [8]. In the study region of this work, the GLM (on GOES-16) detection efficiency for -CG flashes is expected to be about 79 % [9].

^{*} Corresponding author at: New Mexico Institute of Mining and Technology, 801 Leroy Place, Socorro 87801, United States. E-mail address: adonis.leal@nmt.edu (A.F.R. Leal).

Many researchers have investigated -CG processes using electromagnetic fields recorded at ground level [9–17]. Positive CG flashes are relatively rare, but still, there are several studies in which their processes were investigated based on electromagnetic fields recorded on the ground [18–22]. However, most of those studies are limited to relatively small regions (up to a few hundreds of kilometers). The GLM has uniform coverage all over the Americas. Additionally, similar technology has been implemented in Asia (Lightning Mapping Imager - LMI [23]) and Europe/Africa (Lightning Imager - LI [24]). Hence, global-scale studies can now be performed using data from space-borne detectors.

Simultaneous observation of lightning from space and ground were recently performed in Colombia [25-28]. In [25], they observed one negative cloud-to-ground lightning flash at nighttime from the ground with a high-speed camera at 5000 fps and from space by the Modular Multispectral Imaging (MMIA) instrument on the Atmosphere-Space Interactions Monitor (ASIM) (MMIA-ASIM) on the International Space Station (ISS), the Lightning Imaging Sensor also on the ISS (ISS-LIS), and the Geostationary Lightning Mapper (GLM) on GOES-16. They found that GLM reported 3 times higher energy than MMIA-ASIM, and light intensity curves of MMIA-ASIM matched well with those recorded by a high-speed camera at the ground around the time of a return stroke. In [26], MMIA-ASIM, ISS-LIS and GLM observations were complemented by data from the Colombia Lightning Mapping Array (Colombia-LMA) and radar reflectivity products. The main findings in [26] are that surges in radiance at 777.4 nm appear to be related mostly to lightning processes involving hot channels, as well with branching of lightning leaders with new leader development. Additionally, it was found that in cloud areas with reflectivity <18 dBZ above the lightning leader channels at altitudes >7 km, both MMIA-ASIM and GLM detected some emissions. But in the region with reflectivity <23 dBZ above the lightning leader channels, the lightning optical emissions were almost undetectable. In [27], the initiation of four lightning flashes detected from ground by the Colombia-LMA and from space by the MMIA-ASIM, ISS-LIS and GLM was investigated, and in [28] the use of lightning detection from space in electric power systems was explored.

Fairman and Bitzer [29] used the GLM optical attributes associated with each flash to predict the presence of continuing current across the GLM field of view. For North Alabama in the USA, their model had a probability of detection of about 78 % and a false alarm rate of about 6 %. They compared GLM flashes containing continuing current with electric field measurements and high-speed video recordings and concluded that continuing currents can be detected from space by the

GLM, although further research for other regions (beyond North Alabama) is needed.

In this study, we investigate the ability of GLM to detect optical emissions from -CG and +CG lightning processes, including preliminary breakdown pulses (PB), first stroke leaders (FL), return-strokes (RS), and subsequent stroke leaders (SL). To do so, we recorded wideband lightning electric field waveforms using fast and slow antennas in the Amazon, identified time windows of individual lightning processes in those records, and examined the corresponding GLM group data (optical emissions). The results were interpreted in terms of detectability of individual lightning processes by GLM. This is an expanded version of [30], which includes a more robust dataset for -CGs and a new dataset for +CGs.

2. Data and methodology

The lightning electric field waveforms analyzed in this study were recorded using two flat-plate antenna systems (fast and slow) located on the roof of the Lightning Research Laboratory at the Federal University of Para, Brazil (-1.47°, -48.45°, see Fig. 1). The flat-plate antennas were connected to a preamplifier via a 10-m long coaxial cable. The fast antenna system had a decay time constant of about 1 ms, while the slow one had a decay time constant of about 500 ms. The preamplifier consists of an integrator and a unity-gain, low-noise amplifier. The lightning electric field signals were sampled at 5 MHz with a Picoscope. The record length was 2 s with a pretrigger time (time interval between the beginning of the record and the first pulse whose magnitude exceeded the trigger threshold) of 600 ms. A similar setup was used in [9], and the calibration was performed based on [31]. Each event received a GPS timestamp relative to the trigger time. All the electric field waveforms were recorded between May and June of 2022.

The GLM data are organized into three different processing levels, from raw data at level 0 (essentially raw images from the optical sensor) to the final product data at level 2. In this work, we use level 2 data which are divided into event, group, and flash data. An event is defined as a single pixel that exceeds the dynamic background average radiance by a selected margin. Events are the basic data product of GLM. Each of them represents a single cloud top pixel illuminated by lightning during a single time frame (2 ms). A group is a result of two or more adjacent events within the same 2 ms time frame. Groups are intended to be directly related to individual lightning strokes (see Fig. 4 of [5]). A flash consists of one or more groups within 330 ms separated by no more than

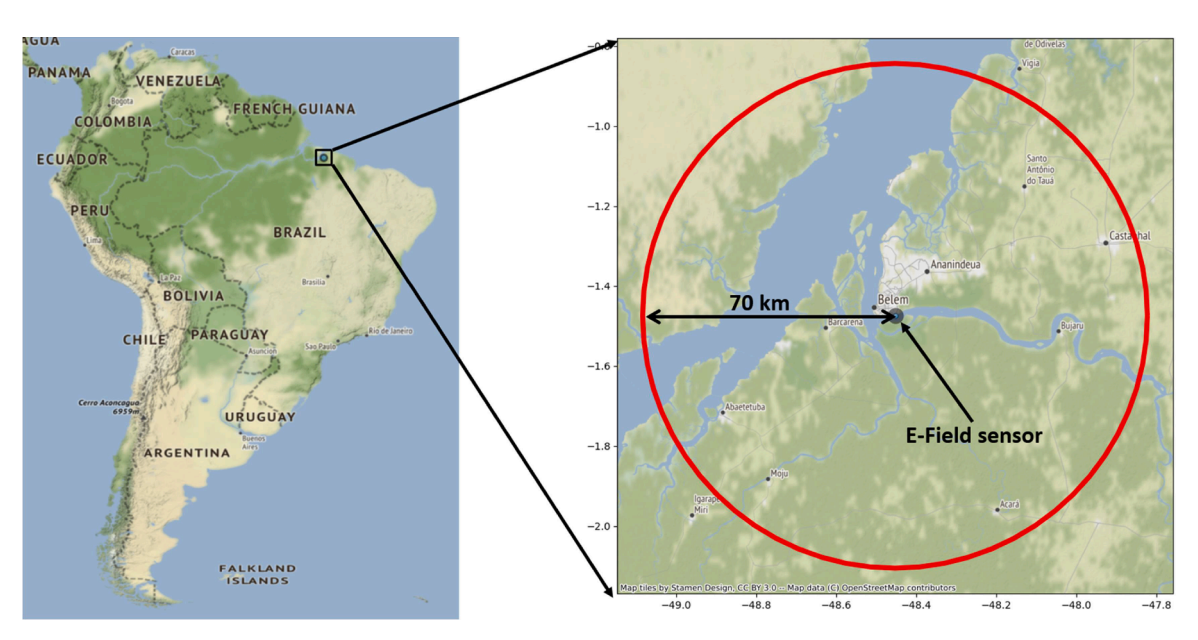


Fig. 1. Study region.

16.5 km from each other. More details on GLM can be found in [5].

We used the GPS timestamp to match the measured E-field waveforms with GLM group data. Fig. 2 shows an example of a -CG flash containing 3 RSs that was simultaneously recorded by the E-field measuring systems at ground level and from space by the GLM. In Fig. 2, we show the lightning electric field records, GLM group energy time series, GLM events and groups location, cloud top brightness temperature (CTBT), and return stroke locations reported by Earth Networks Total Lightning Network (ENTLN). In Supplementary Material, we show similar figures for all flashes examined in this study.

3. Results and discussion

We examined the GLM detection efficiency for four lightning processes in both positive and negative CGs: preliminary breakdown (PB), first-stroke leaders (FL), subsequent-stroke leaders (SL), and return

strokes (RS). First, we inspected the electric field waveforms in order to identify PB (if any) and count the number of RSs in each flash. Second, we plotted on the same time scale the GLM group energy and E-field waveforms, in order to find GLM groups related to PB, FL, SL, and RS. Table 1 summarizes the results for -CGs and Table 2 for +CGs. The mean values of the number of strokes per flash, distance, and E-field peak normalized to 100 km for -CGs were 3.7, 10 km, and 3.5 V/m, and for +CGs they were 1.6, 33 km, and 12 V/m. Thus, +CG return strokes examined in this study were a factor of 3 to 4 more intense than their -CG counterparts.

It is important to note that, in the present study, whenever we state that GLM detected any particular lightning process, we refer to light emissions detected from space, which are produced by any channel or channels (both inside and outside the cloud) during the time window of that process, with this window being identified in the corresponding record from the ground-based electric field sensor.

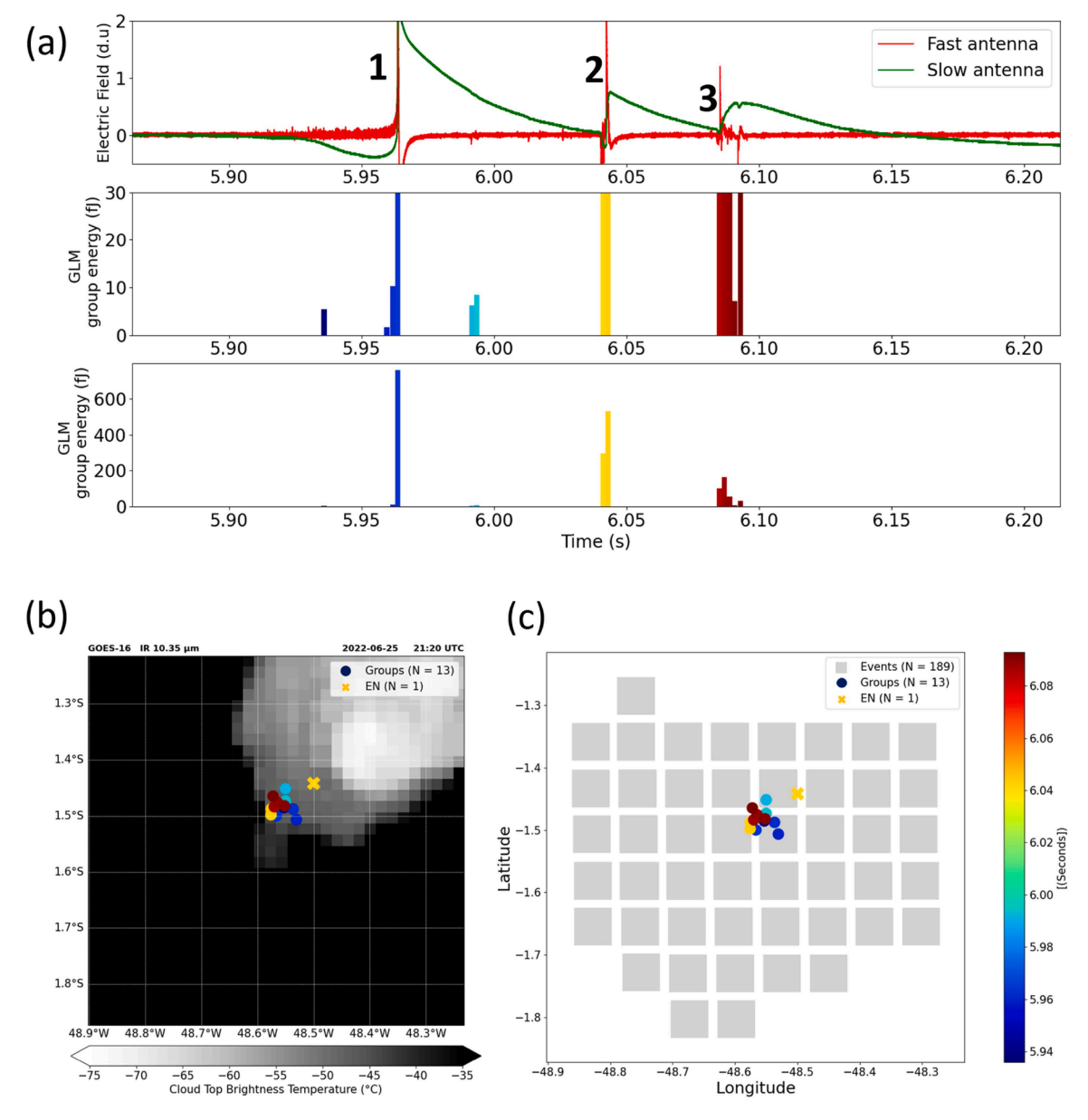


Fig. 2. A -CG flash that occurred 13 km from the E-field measuring system. The flash contained 3 return strokes (numbered in the top panel) all of which were also recorded by the GLM. Only the second stroke was detected by the ENTLN. (a) top panel, lightning electric field records (fast and slow), middle panel, GLM groups in the 0 to 30 fJ range to accentuate small energy groups, and bottom panel, GLM groups in the full energy range. fJ stands for femtojoule; $1 \text{fJ} = 10^{-15} \text{ J}$. GLM group energy are colored by time to comparison with the spatial plot. (b) GLM groups, and ENTLN reported locations of return strokes (in this case only one stroke), and cloud top brightness temperature in the background. (c) GLM groups, GLM events, and ENTLN reported locations of return strokes.

Table 1Summary of data and results for 15 negative CGs.

Flash ID	Number of strokes	Distance (km)	E-field peak at 100 km (V/m)	Detectable PB in E- field	PB- GLM	FL- GLM	RS detected by GLM	SL- GLM	Local time (H: M)
2	1	8.7	2.1	YES	YES	YES	ALL	-	16:59
3	6	13.7	5.5	YES	YES	YES	ALL	YES (3)	17:00
4	1	3.8	0.6	YES	YES	YES	ALL	-	17:06
7	5	7.3	2.9	YES	NO	NO	4	NO	17:11
9	6	9.3	1.7	YES	NO	NO	5	NO	17:14
10	1	5.1	1.2	YES	YES	YES	ALL	-	17:15
11	5	10.7	3.3	YES	NO	YES	ALL	YES (3)	17:18
12	4	11.1	4.0	YES	NO	NO	ALL	YES (2)	17:19
14	1	11.8	3.4	YES	NO	NO	ALL	-	18:28
142	3	15.3	2.3	YES	NO	NO	ALL	YES (1)	18:01
143	5	15.1	1.9	YES	NO	NO	ALL	YES (2)	18:03
151	1	10.8	6.5	YES	NO	NO	ALL	-	18:19
152	10	6.6	3.0	YES	NO	NO	7	YES (3)	18:20
153	3	13	8.1	YES	YES	YES	ALL	YES (2)	18:23
154	4	14	6.4	YES	NO	NO	3	NO	18:24

PB-GLM, Did the GLM detect any PB pulses?

FL-GLM. Did the GLM detect the first-stroke leader?

SL-GLM, Did the GLM detect any subsequent-stroke leaders?

Table 2 Summary of data and results for 15 positive CGs.

Flash	Number of	Distance	E-field peak at 100 km	Detectable PB in E-	PB-	FL-	RS detected by	SL-	Local time (H:
ID	strokes	(km)	(V/m)	field	GLM	GLM	GLM	GLM	M)
82	2	37.4	23.6	YES	YES	NO	ALL	YES (1)	16:08
106	1	17.2	7.3	YES	YES	YES	ALL	-	20:04
117	1	19.7	7.8	YES	YES	YES	ALL	-	20:25
119	1	40	11.0	YES	YES	YES	ALL	-	16:49
338	2	13.4	11.9	YES	YES	NO	1	NO	19:03
365	3	62.9	24.2	YES	YES	YES	ALL	YES (2)	19:32
369	1	15	7.2	YES	YES	YES	ALL	-	19:39
371	1	56	11.2	YES	YES	YES	ALL	-	19:40
377	2	68.3	13.8	YES	YES	NO	ALL	YES (1)	19:51
379	2	15	12.5	YES	YES	YES	ALL	YES (1)	19:55
380	1	23.5	8.1	YES	YES	YES	ALL	-	19:57
382	3	22.2	20.2	YES	YES	YES	ALL	YES (2)	20:03
386	1	15.7	2.0	YES	YES	YES	ALL	-	20:15
388	1	67.34	15.2	YES	YES	YES	ALL	-	20:18
389	2	26	4.1	YES	YES	YES	ALL	YES (1)	20:26

PB-GLM, Did the GLM detect any PB pulses?

FL-GLM, Did the GLM detect the first-stroke leader?

SL-GLM, Did the GLM detect any subsequent-stroke leaders?

3.1. Preliminary breakdown (PB)

In all +CG and -CG flashes we observed electric field signatures of PB (preliminary breakdown pulses). GLM detected all PBs in positive flashes and 53 % in negative flashes. Stolzenburg et al. [32] observed optical emissions from PB at ground level using high-speed cameras. Most of their optical emissions from PB were weak, but still detectable from ground level. López et al. [27] simultaneously observed the initiation of four lightning flashes from space and the ground using MMIA-ASIM, ISS-LIS, GLM, and Colombia-LMA. In three of their four flashes, red emissions (777.4 nm), the same line that GLM operates at, were not detected during their initiation. In these cases, the initiation was accompanied by bipolar VLF/LF waveform with a short duration (<40 µs). However, blue emissions (337 nm) were detected. In this study, the GLM detection efficiency for PB in -CGs (53 %) was considerably lower than that in +CGs (100 %). There are two possible explanations for this disparity: (1) relatively weak (in most cases) amplitudes of electric field signatures of PB in -CGs and (2) the stronger scattering of optical emission from PB in -CGs by the thundercloud which makes them difficult to be observed from space. Indeed, the preliminary breakdown in -CGs usually occurs near the bottom of the thundercloud, and because of that, optical signals experience more scattering than in the case of +CGs. Specifically, in the Amazon region, where we have deep thunderclouds, we believe that the thickness of the cloud often does not allow the detectable luminosity originating near the cloud bottom to reach the GLM sensor. However, in 4 out of 9 flashes that GLM did not detect light emission related to PB pulses, the flashes seem to occur in a not so thick region of the cloud, as inferred from relatively high CTBT. Figures with GLM events and groups location, and CTBT for all flashes are found in Supplementary Material.

Fig. 3 shows one example of a PB whose light emission was not detected by the GLM. Fig. 4 shows two examples (-CG and +CG) of electric field signatures of PB whose light emission was detected by GLM. It is interesting to note the difference in the magnitudes of GLM groups energy related to PB and to RS. For -CG shown in Fig. 4 (a), the energy from the groups related to RS is about 100 times higher than the energy from the groups related to PB, while for +CG shown in Fig. 4 (b), the difference is considerably smaller (about a factor of 25).

3.2. First-stroke leaders (FL)

For negative CG flashes, GLM detected light emissions of the first

^{*}Sunset at 18:15 (Local time) at E-field sensor location.

^{*}Sunset at 18:15 (Local time) at E-field sensor location.

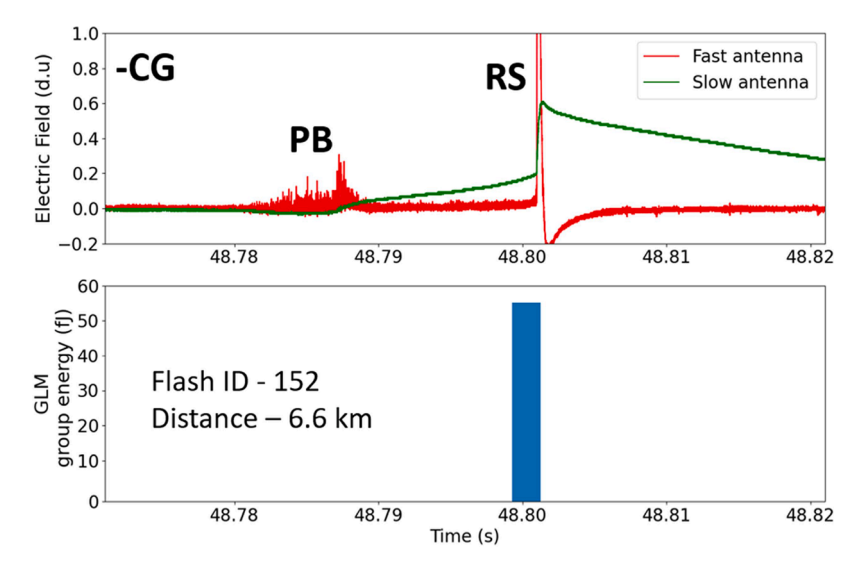


Fig. 3. E-field waveforms of the first return stroke preceded by the preliminary breakdown (PB) pulses in -CG flash 152 and the corresponding GLM group energy record. Note that PB was not detected by GLM.

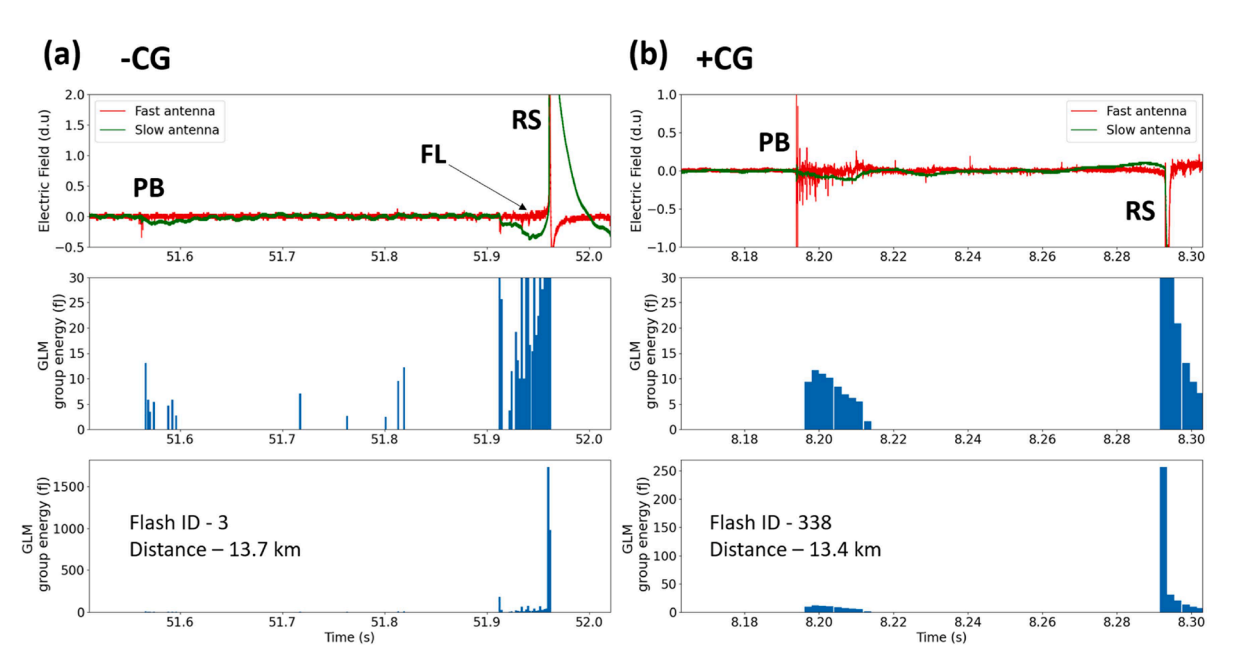


Fig. 4. E-field waveforms of first return strokes preceded by preliminary breakdown (PB) pulses in (a) negative and (b) positive CG flashes and the corresponding GLM group energy records.

stepped leader in 53 % (8 out of 15) of the flashes. For positive CG flashes, GLM detected the first leader in 80 % (12 out of 15) of the flashes. We assumed that GLM detected FL if it detected at least one group prior to the first return stroke group. One example of GLM-detected FL in a negative CG flash is seen in Fig. 4 (a).

The energy of GLM groups that are related to FLs is lower than for groups related to RSs, for both negative and positive flashes. For flashes 153 and 106 shown in Fig. 5 (a) and (b), respectively, it is interesting to note that the group energy increases with time. Perhaps this is because of the elongation of the leader channel branches developing outside the cloud, which allowed more energy to reach the optical sensor of GLM.

3.3. Subsequent-stroke leaders (SL)

Out of 41 subsequent return strokes in negative CG flashes we observed GLM groups related to subsequent-stroke leaders in 16 (39 %) cases (see the last column of Table 1). For positive subsequent return

strokes, we observed GLM groups in 8 out of 9 (89 %) cases (see the last column of Table 2). We defined an SL as detected by GLM if it detected at least one group prior to the corresponding subsequent return stroke group. The lower percentage of detection of SL in negative flashes by GLM can be related to their relatively low intensity. Fig. 6 shows the second RSs in negative and positive flashes, for which GLM groups related to E-field signatures (labeled SL) prior to the RS can be seen. Again, it is important to note that the energy of the groups related to SL in both positive and negative flashes is much lower than that of groups related to RS.

3.4. Return strokes (RS)

The RS is the most powerful process in a CG lightning flash, and this is why the GLM was able to detect most of the return strokes that we recorded by the electric field sensor at ground level. Boggs et al. [33], using a high-speed optical spectrograph, observed a peak at 777.4 nm in

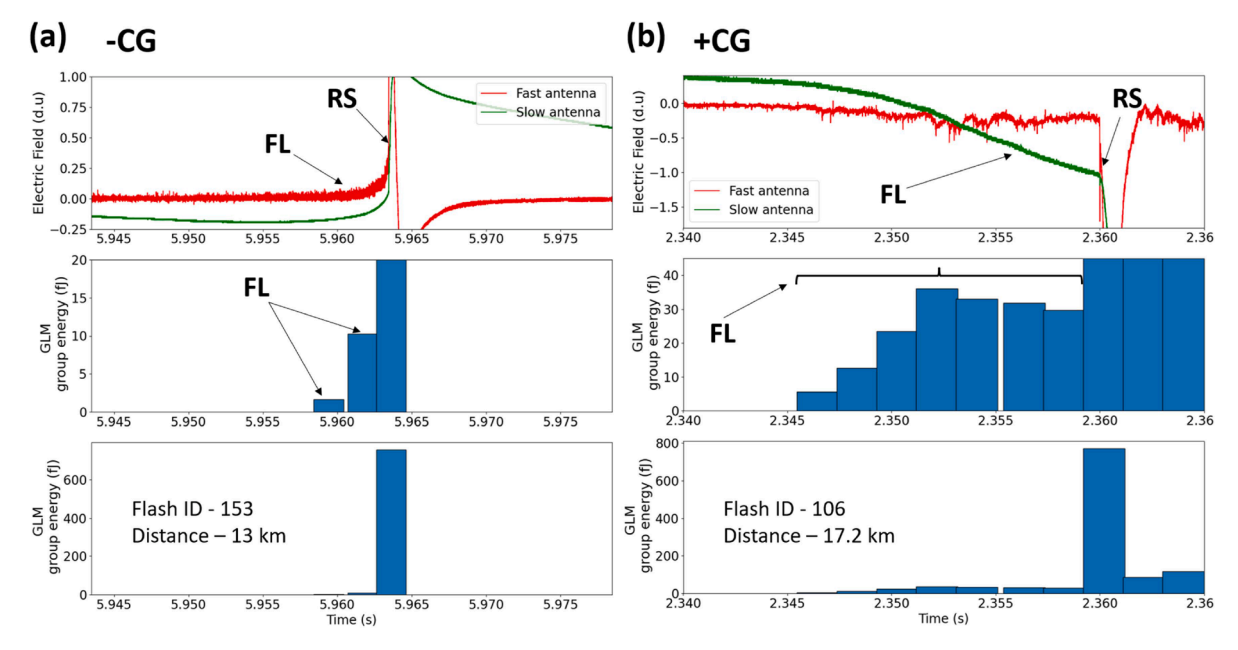


Fig. 5. E-field waveforms of first return strokes preceded by first leaders in (a) negative and (b) positive flashes and the corresponding GLM group energy records.

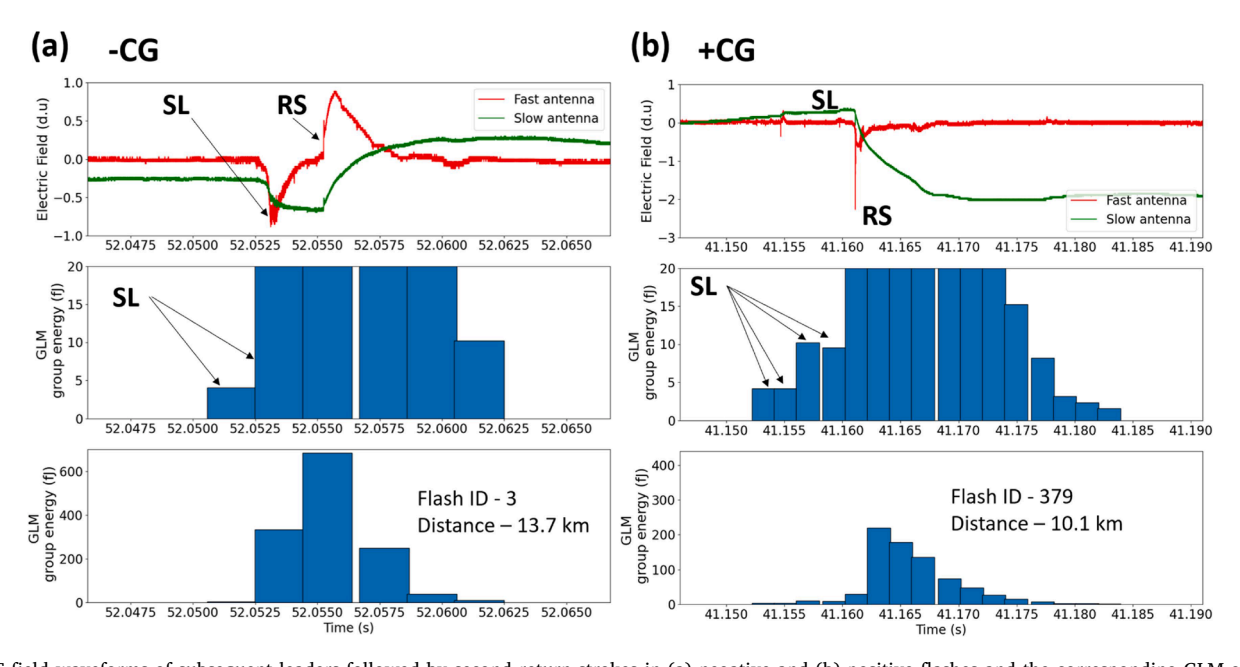


Fig. 6. E-field waveforms of subsequent leaders followed by second return strokes in (a) negative and (b) positive flashes and the corresponding GLM group energy records.

the return-stroke spectrum, and it is the same wavelength at which the GLM sensor operates. It is worth noting, however, that all hot lightning channels (including leaders and continuing currents) are expected to radiate at 777.4 nm. We observed that only the RSs with relatively low electric field amplitude (normalized to 100 km) were missed by GLM.

We investigated the sustained optical emissions after the onset time of each RS in order to find flashes containing continuing currents and M-components. To do so, we computed the number of GLM groups, with no frame gaps (<1 frame gap between groups), after the onset time of each return stroke. Table 3 summarizes the statistics on the number of GLM groups per RS. The average number of groups in negative RS is 1.6 which is considerably lower than that for positive RS (15.8). If we multiply these numbers by the GLM frame duration (2 ms) we find that the average sustained optical emission for negative RSs is 3.2 ms versus 31.6 ms for positive RSs. About 26 % (6 out of 23) of positive RSs were

Table 3 Statistics on the number of GLM groups per return stroke for -CG and +CG flashes.

	Min	Max	Mean	SD
-CG	1	8	1.6	1.2
+CG	1	85	15.8	19

followed by optical emissions characteristic of long-continuing-current (LCC). LCCs are usually defined as those having a duration of more than 40 ms ([1], ch. 4). No negative RSs in this study were followed by sustained optical emissions longer than 40 ms. One positive flash (see 386 in Table 2) had a sustained optical emission that lasted for about 170 ms after the return stroke, and it was the longest LCC in our dataset.

Data for this flash are shown in Fig. 7(b).

We observed variations in GLM group energy resembling M-components after the RS in 6 +CG flashes. No such variations were observed in -CG flashes. M-components are defined as perturbations superimposed on the slowly varying lightning current, which are accompanied by enhancements in the lightning channel luminosity ([1], ch. 4). They are well studied in -CG flashes, where their typical durations are a few milliseconds. Fig. 7 shows examples of two positive RSs followed by pronounced luminosity variations that occurred during long continuing currents. We tentatively labeled those luminosity variations as M-components, although their durations (up to tens of milliseconds) are considerably longer than those of "classical" M-components in -CG flashes. Note that most of the M-components labeled in Fig. 7 appear to be accompanied by electric field variations and, hence, cannot be attributed to the varying exposure of continuing current channel to the GLM optical sensor. There is little information in the literature on Mcomponent-type processes in +CG flashes (see [34]). Further research is needed to understand the nature of large luminosity humps seen in Fig. 7. We wonder if they could be accompanied by the so-called delayed sprites (e.g., [35,36]).

4. Summary

In this work, we recorded wideband lightning electric field waveforms in the Amazon and compared them with the corresponding GLM group data (optical energy) to investigate what lightning processes can be detected, via their optical emissions at 777.4 nm, from space by GLM. Based on a sample of 15 -CG flashes containing 56 strokes and 15 +CG flashes containing 24 strokes, we found that GLM detected more than 90 % of all return strokes in our dataset. GLM missed more RSs in -CGs than in +CGs, and the missed RSs had relatively small electric field peaks (and by inference current peaks). Preliminary breakdown processes were detected by GLM in 100 % of +CGs and in 53 % of -CGs. Further, GLM detected 60 % of all first-stroke leaders (+CGs and -CGs combined). GLM detection efficiency for subsequent-stroke leaders was 39 % for -CGs and 89 % for +CGs. It was found that positive RSs were associated with longer sustained optical emissions 31.6 ms versus 3.2 ms for negative RS. About 26 % of positive RSs were followed by optical emissions characteristic of long (>40 ms) continuing current that exhibited previously unreported large variations resembling M-components. Our findings can help future efforts to distinguish between -CG and +CG flashes and improve the methodologies to track hazardous lightning flashes with continuing currents from space.

CRediT authorship contribution statement

Adonis F.R. Leal: Conceptualization, Data curation, Formal analysis, Funding acquisition, Investigation, Methodology, Software, Supervision, Visualization, Writing – original draft, Writing – review & editing. Vladimir A. Rakov: Data curation, Formal analysis, Funding

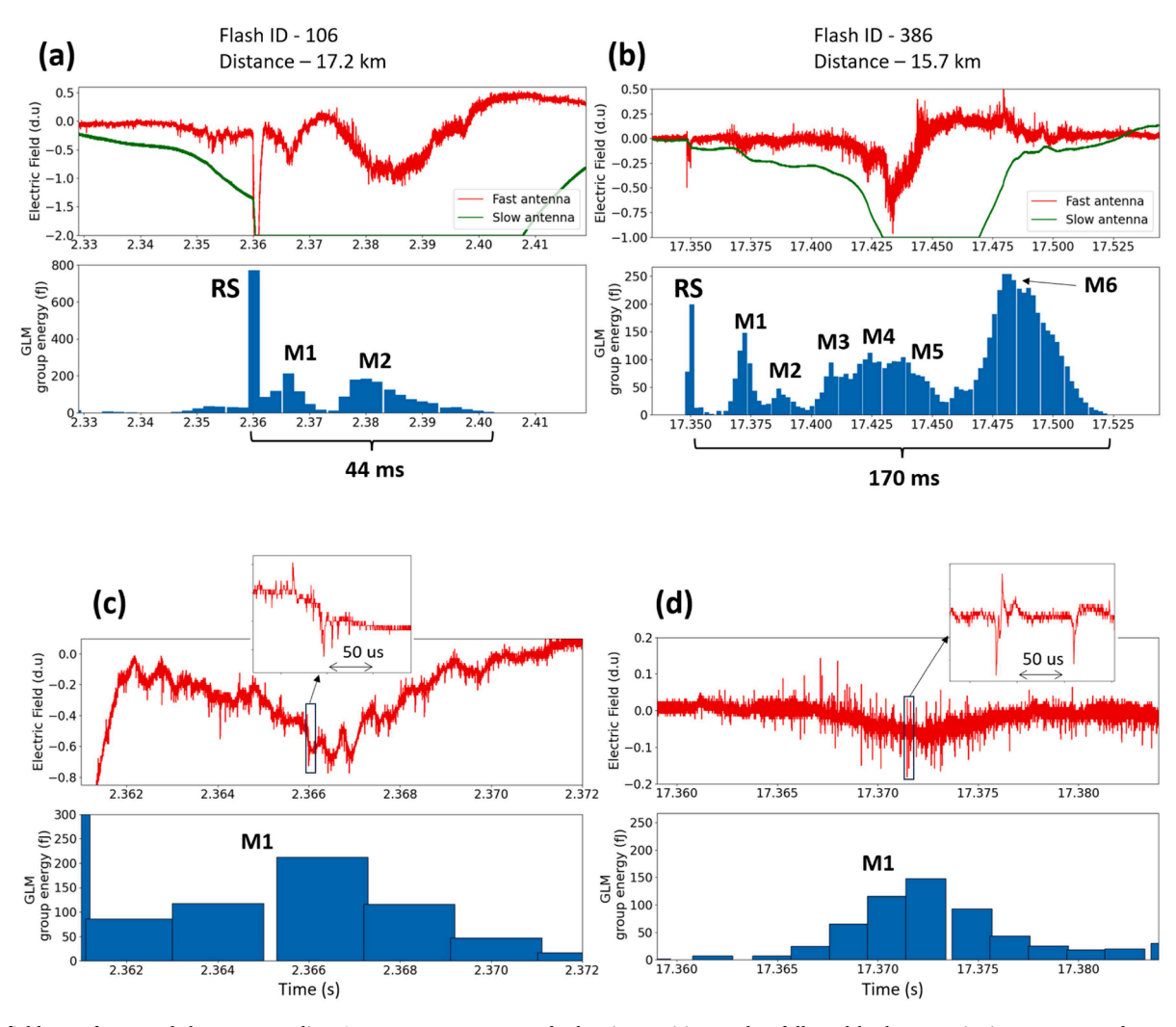


Fig. 7. E-field waveforms and the corresponding GLM group energy records showing positive strokes followed by long continuing currents and pronounced luminosity variations resembling M-components. (c) and (d) are the expansions of (a) and (b), respectively.

acquisition, Supervision, Writing - original draft, Writing - review & editing.

Declaration of competing interest

The authors declare that they have no known competing financial interests or personal relationships that could have appeared to influence the work reported in this paper.

Data availability

Data will be made available on request.

Acknowledgment

A special thanks goes to Marcio Lopes for provide the code to download cloud top brightness temperature from GOES-16. This work was supported in part by the National Council for Scientific and Technological Development (CNPq) grant 407250/2021-2 and NSF grant AGS - 2055178.

Supplementary materials

Supplementary material associated with this article can be found, in the online version, at doi:10.1016/j.epsr.2024.110183.

References

- [1] V.A. Rakov, M.A. Uman, Lightning: Physics and Effects, Cambridge University Press, New York, 2003, https://doi.org/10.1017/CBO978110734088
- [2] V.A. Rakov, Fundamentals of Lightning, Cambridge University Press, New York, 2016, https://doi.org/10.1017/CBO978113968037
- T. Neubert, et al., The ASIM mission on the international space station, Space Sci. Rev. 215 (2) (2019) 26, https://doi.org/10.1007/s11214-019-0592-z. Mar.
- [4] J. Wemhoner, et al., Lightning radiometry in visible and infrared bands, Atmos. Res. 292 (2023) 106855, https://doi.org/10.1016/j.atmosres.2023.106855. Sep.
- [5] S.J. Goodman, et al., The GOES-R geostationary lightning mapper (GLM), Atmos. Res. 125-126 (2013) 34-49, https://doi.org/10.1016/j.atmosres.2013.01.006
- [6] S.D. Rudlosky, S.J. Goodman, K.S. Virts, E.C. Bruning, Initial geostationary lightning mapper observations, Geophys. Res. Lett. 46 (2) (2019) 1097-1104, https://doi.org/10.1029/2018GL081052. Jan.
- [7] D. Zhang, K.L. Cummins, Time evolution of satellite-based optical properties in lightning flashes, and its impact on GLM flash detection, J. Geophys. Res. Atmos. 125 (6) (Mar. 2020), https://doi.org/10.1029/2019JD032024.
- [8] M. Bateman, D. Mach, M. Stock, Further investigation into detection efficiency and false alarm rate for the geostationary lightning mappers aboard GOES-16 and GOES-17, Earth Space Sci. 8 (2) (2021), https://doi.org/10.1029/2020EA001237.
- [9] A. Leal, W. Matos, E. Ferreira, G. Ferreira, M. Lopes, B. Rocha, Characteristics of negative cloud-to-ground flashes observed in the Brazilian amazon region, J. Geophys. Res. Atmos. (2021), https://doi.org/10.1029/2020JD034492. Jul.
- [10] A. Leal, V. Rakov, Characterization of lightning electric field waveforms using a large database: 1. methodology, IEEE Trans. Electromagn. Compat. 63 (4) (2021) 1155-1162, https://doi.org/10.1109/TEMC.2021.3059266. Aug.
- [11] A.F.R. Leal, V.A. Rakov, Characterization of lightning electric field waveforms using a large database: 2. analysis and results, IEEE Trans. Electromagn. Compat. (2021) 1-9, https://doi.org/10.1109/TEMC.2021.3062172
- [12] C.L. Wooi, Z. Abdul-Malek, N.A. Ahmad, A.I. El Gayar, Statistical analysis of electric field parameters for negative lightning in Malaysia, J. Atmos. Sol. Terr. Phys. 146 (2016) 69-80, https://doi.org/10.1016/j.jastp.2016.05.007. Aug.
- [13] B. Zhu, M. Ma, W. Xu, D. Ma, Some properties of negative cloud-to-ground flashes from observations of a local thunderstorm based on accurate-stroke-count studies, J. Atmos. Sol. Terr. Phys. 136 (2015) 16-22, https://doi.org/10.1016/j jastp.2015.07.007. Dec.

- [14] M.A. Haddad, V.A. Rakov, S.A. Cummer, New measurements of lightning electric fields in Florida: waveform characteristics, interaction with the ionosphere, and peak current estimates, J. Geophys. Res. Atmos. 117 (D10) (2012), https://doi.org/ 10.1029/2011JD017196 n/a-n/aMay.
- [15] Z.A. Baharudin, N.A. Ahmad, J.S. Mäkelä, M. Fernando, V. Cooray, Negative cloudto-ground lightning flashes in Malaysia, J. Atmos. Sol. Terr. Phys. 108 (Feb. 2014) 61-67, https://doi.org/10.1016/j.jastp.2013.12.001.
- [16] V.A. Rakov, M.A. Uman, Waveforms of first and subsequent leaders in negative lightning flashes, J. Geophys. Res. 95 (D10) (1990) 16561, https://doi.org/ 10.1029/JD095iD10p16561.
- [17] V. Cooray, K.P.S.C. Jayaratne, Characteristics of lightning flashes observed in Sri Lanka in the tropics, J. Geophys. Res. 99 (D10) (1994) 21051, https://doi.org/
- [18] X.M. Shao, C.T. Rhodes, D.N. Holden, RF radiation observations of positive cloudto-ground flashes, J. Geophys. Res. Atmos. 104 (D8) (1999) 9601-9608, https:// doi.org/10.1029/1999JD900036. Apr.
- [19] A. Nag, V.A. Rakov, Positive lightning: an overview, new observations, and inferences, J. Geophys. Res. Atmos. 117 (D8) (2012), https://doi.org/10.1029/ 2012JD017545 n/a-n/aApr.
- [20] A. Nag, V.A. Rakov, Parameters of electric field waveforms produced by positive lightning return strokes, IEEE Trans. Electromagn. Compat. 56 (4) (2014) 932-939, https://doi.org/10.1109/TEMC.2013.2293628. Aug.
- A. Hazmi, P. Emeraldi, M. Hamid, N. Takagi, D. Wang, Characterization of positive cloud to ground flashes observed in Indonesia, Atmosphere 8 (1) (2017) 4, https:// doi.org/10.3390/atmos8010004 (Basel)Jan.
- [22] S. Li, S. Qiu, L. Shi, Y. Li, Broadband VHF observations of two natural positive cloud-to-ground lightning flashes, Geophys. Res. Lett. 47 (11) (2020), https://doi. org/10.1029/2019GL086915. Jun.
- [23] J. Yang, Z. Zhang, C. Wei, F. Lu, Q. Guo, Introducing the new generation of Chinese geostationary weather satellites, fengyun-4, Bull. Am. Meteorol. Soc. 98 (8) (2017) 1637–1658, https://doi.org/10.1175/BAMS-D-16-0065.1. Aug.
- [24] R. Stuhlmann, et al., Plans for EUMETSAT's third generation meteosat geostationary satellite programme, Adv. Space Res. 36 (5) (2005) 975-981, https://doi.org/10.1016/j.asr.2005.03.091. Jan.
- O.A. van der Velde, et al., Comparison of high-speed optical observations of a lightning flash from space and the ground, Earth Space Sci. 7 (10) (2020), https:// doi.org/10.1029/2020EA001249. Oct.
- [26] J. Montanyà, et al., A simultaneous observation of lightning by ASIM, Colombialightning mapping array, GLM, and ISS-LIS, J. Geophys. Res. Atmos. 126 (6) (2021), https://doi.org/10.1029/2020JD033735, Mar.
- [27] J.A. López, et al., Initiation of lightning flashes simultaneously observed from space and the ground: Narrow bipolar events, Atmos. Res. 268 (2022) 105981, https://doi.org/10.1016/j.atmosres.2021.105981. Apr.
- [28] J. Montanyà, et al., Potential use of space-based lightning detection in electric power systems, Electric Power Syst. Res. 213 (2022) 108730, https://doi.org/ 10.1016/j.epsr.2022.108730. Dec.
- S.I. Fairman, P.M. Bitzer, The detection of continuing current in lightning using the geostationary lightning mapper, J. Geophys. Res. Atmos. 127 (5) (2022), http doi.org/10.1029/2020JD033451. Mar.
- [30] A.F.R. Leal, V.A. Rakov, Processes in -CG lightning flashes detected from space by GLM: A ground-truth study in the Amazon, in: Proceedings of the 2022 36th International Conference on Lightning Protection (ICLP), IEEE, 2022, pp. 329-332, ottps://doi.org/10.1109/ICLP56858.2022.9942614. Oct.
- [31] A.F.R. Leal, V.A. Rakov, J. Pissolato Filho, B.R.P. Rocha, M.D. Tran, A low-cost system for measuring lightning electric field waveforms, its calibration and application to remote measurements of currents, IEEE Trans. Electromagn. Compat. 60 (2) (2018) 414-422, https://doi.org/10.1109/TEMC.2017.2723524.
- [32] M. Stolzenburg, et al., Luminosity of initial breakdown in lightning, J. Geophys.
- Res. Atmos. 118 (7) (2013) 2918–2937, https://doi.org/10.1002/jgrd.50276. Apr. [33] L.D. Boggs, et al., Vertical temperature profile of natural lightning return strokes derived from optical spectra, J. Geophys. Res. Atmos. 126 (8) (2021), https://doi. g/10.1029/2020JD034438. Apr.
- [34] Z. Ding, V.A. Rakov, Y. Zhu, M.D. Tran, I. Kereszy, Transient phenomena in positive cloud-to-ground lightning discharges, Commun. Phys. 5 (1) (2022) 313, ttps://doi.org/10.1038/s42005-022-01087-8. Dec
- [35] S.A. Yashunin, E.A. Mareev, V.A. Rakov, Are lightning M components capable of initiating sprites and sprite halos? J. Geophys. Res. Atmos. 112 (D10) (2007) https://doi.org/10.1029/2006JD007631. May.
- [36] L. Contreras-Vidal, et al., Relationship between sprite current and morphology, J. Geophys. Res. Space Phys. 126 (3) (2021), https://doi.org/10.1029. 2020JA028930. Mar.